



HAL
open science

Regulation of PPAR α by APP in Alzheimer disease impacts the pharmacological modulation of synaptic activity

Francisco Sáez-Orellana, Thomas Leroy, Floriane Ribeiro, Anna Kreis, Karelle Leroy, Fanny Lalloyer, Eric Baugé, Bart Staels, Charles Duyckaerts, Jean-Pierre Brion, et al.

► To cite this version:

Francisco Sáez-Orellana, Thomas Leroy, Floriane Ribeiro, Anna Kreis, Karelle Leroy, et al.. Regulation of PPAR α by APP in Alzheimer disease impacts the pharmacological modulation of synaptic activity. JCI Insight, 2021, 10.1172/jci.insight.150099 . hal-03280763

HAL Id: hal-03280763

<https://hal.sorbonne-universite.fr/hal-03280763>

Submitted on 7 Jul 2021

HAL is a multi-disciplinary open access archive for the deposit and dissemination of scientific research documents, whether they are published or not. The documents may come from teaching and research institutions in France or abroad, or from public or private research centers.

L'archive ouverte pluridisciplinaire **HAL**, est destinée au dépôt et à la diffusion de documents scientifiques de niveau recherche, publiés ou non, émanant des établissements d'enseignement et de recherche français ou étrangers, des laboratoires publics ou privés.



Distributed under a Creative Commons Attribution 4.0 International License

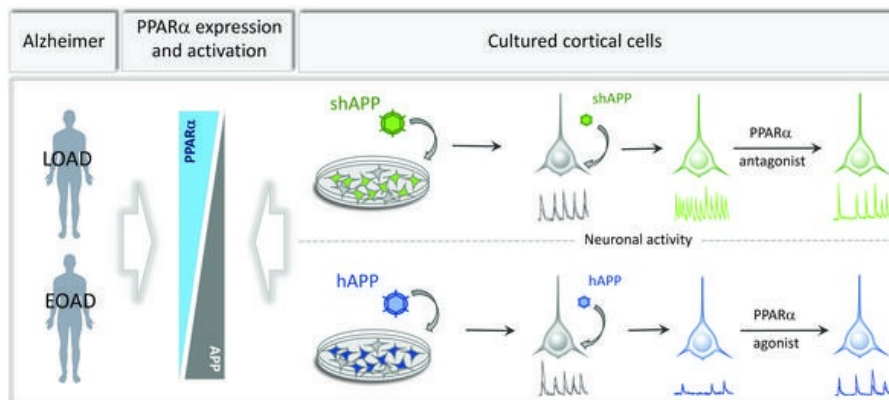
Regulation of PPAR α by APP in Alzheimer disease impacts the pharmacological modulation of synaptic activity

Francisco Sáez-Orellana, ... , Jean-Noël Octave, Nathalie Pierrot

JCI Insight. 2021. <https://doi.org/10.1172/jci.insight.150099>.

Research In-Press Preview Neuroscience

Graphical abstract



Find the latest version:

<https://jci.me/150099/pdf>



1 **Title:**

2 **Regulation of PPAR α by APP in Alzheimer disease impacts the pharmacological**
3 **modulation of synaptic activity.**

4

5

6 **Authors and affiliations:**

7 Francisco Sáez-Orellana^{1†}, Thomas Leroy¹, Floriane Ribeiro¹, Anna Kreis², Karelle Leroy³,
8 Fanny Lalloyer⁴, Eric Baugé⁴, Bart Staels⁴, Charles Duyckaerts⁵, Jean-Pierre Brion³, Philippe
9 Gailly², Jean-Noël Octave¹ and Nathalie Pierrot^{1,†,*}.

10

11 ¹ Université catholique de Louvain, Institute of Neuroscience, Alzheimer Dementia group, B-
12 1200 Brussels, Belgium.

13 ² Université catholique de Louvain, Institute of Neuroscience, Laboratory of Cell Physiology,
14 B-1200 Brussels, Belgium.

15 ³ Université libre de Bruxelles, Laboratory of Histology and Neuropathology, 1070 Brussels,
16 Belgium.

17 ⁴ Univ. Lille, Inserm, CHU Lille, Institut Pasteur de Lille, U1011, F-59000 Lille, France.

18 ⁵ Sorbonne Université, Hôpital de la Pitié-Salpêtrière, Paris Brain Institute (ICM), CNRS
19 UMR7225, INSERM U1127, 75013 Paris, France.

20 † These authors contributed equally to this work.

21 * Correspondence: Nathalie Pierrot, Université catholique de Louvain, Institute of
22 Neuroscience, Alzheimer Dementia, avenue Mounier 53, SSS/IONS/CEMO-Bte B1.53.03, B-
23 1200, Brussels, Belgium. Office: +32 2 764 93 34, E-mail: nathalie.pierrot@uclouvain.be

24

25 Thomas Leroy's present affiliation: VIB Center for Brain and Disease Research & KU Leuven,
26 Department of Neurosciences, Gasthuisberg, B-3000 Leuven, Belgium

27

28

29

30

31 **Conflict of interest statement:**

32 The authors have declared that no conflict of interest exists.

33

34

37 **Abstract**

38 Among genetic susceptibility loci associated with late-onset Alzheimer disease (LOAD),
39 genetic polymorphisms identified in genes encoding lipid carriers led to the hypothesis that a
40 disruption of lipid metabolism could promote disease progression. We previously reported that
41 amyloid precursor protein (APP) involved in AD pathophysiology impairs lipid synthesis
42 needed for cortical networks activity and that activation of peroxisome proliferator-activated
43 receptor α (PPAR α), a metabolic regulator involved in lipid metabolism, improves synaptic
44 plasticity in an AD mouse model. These observations led us to investigate a possible correlation
45 between PPAR α function and full-length APP expression. Here, we report that PPAR α
46 expression and activation are inversely related to APP expression both in LOAD brains and in
47 early-onset AD cases with a duplication of the *APP* gene, but not in control human brains.
48 Moreover, human APP expression decreased *PPARA* expression and its related target genes in
49 transgenic mice and in cultured cortical cells, while opposite results were observed in APP
50 silenced cortical networks. In cultured neurons, APP-mediated decrease or increase in synaptic
51 activity was corrected by PPAR α specific agonist and antagonist, respectively. APP-mediated
52 control of synaptic activity was abolished following PPAR α deficiency, indicating a key
53 function of PPAR α in this process.

54

55

56 **Introduction**

57

58 Alzheimer's disease (AD) is the most common form of dementia, accounting for nearly 70%
59 of the cases worldwide (1). AD is characterized by the presence in the brain of neurofibrillary
60 tangles containing paired helical filaments of hyper-phosphorylated tau protein and senile
61 plaques, with an amyloid core of amyloid β ($A\beta$) peptide derived from the amyloid precursor
62 protein (APP) (2). Synaptic dysfunction seems to occur long before the presence of these
63 neuropathological lesions in the brain of AD patients and might contribute to cognitive
64 dysfunction (3). Autosomal dominant mutations found in *APP* gene or genes encoding
65 presenilins, involved in the γ -secretase-mediated processing of APP into $A\beta$, account for the
66 majority of rare inherited early-onset AD cases (EOAD), in which $A\beta$ is considered as the main
67 culprit of the pathology (1). However, genome-wide association studies have identified dozens
68 of genetic susceptibility loci that are associated with higher risk for late-onset AD (LOAD) (4).
69 Among the most important AD genetic risk factors, genetic polymorphisms found first in *APOE*
70 and later in *CLU* and *ABCA7* genes encoding lipid carriers (4), led to the hypothesis that a
71 disruption of lipid metabolism could promote disease progression (5). This hypothesis is
72 sustained by findings reporting that genetic polymorphisms in *SREBF* and *PPARA* genes,
73 involved in cholesterol and fatty acid (FA) metabolism, were associated with an increased risk
74 of LOAD (6-8), although the association between the genetic polymorphism identified in
75 *PPARA* encoding the Peroxisome Proliferator-Activated Receptor α ($PPAR\alpha$) and AD is
76 controversial (9). However, several LOAD genetic risk factors are involved in pathways that
77 are governed by $PPAR\alpha$, highlighting a potential link between $PPAR\alpha$ and the etiology of AD
78 (reviewed in (10)). $PPAR\alpha$ belongs to the nuclear receptor superfamily of ligand-dependent
79 transcription factors and is broadly implicated in a wide variety of biological processes
80 regulating energy balance, inflammation, FA and glucose metabolism (11), a set of pathways

81 previously reported to be also disturbed in LOAD (12-14). More recently, a potential role of
82 PPAR α in cognition emerged. Spatial learning and long-term memory deficits observed in
83 PPAR α -knockout mice indicate that PPAR α is required for normal cognitive function (15).
84 Moreover, PPAR α deficiency affects the expression of a set of synaptic-related proteins
85 involved in excitatory neurotransmission (16) and severely impairs hippocampal long-term
86 potentiation (LTP) (17), an activity-dependent enhancement of synaptic strength involved in
87 memory processing (18). Accordingly, a growing body of evidence reports that activation of
88 PPARs has salutary effects on neurodegenerative disorders including AD (19). Administration
89 of PPAR α activators reduces AD-like pathology and cognitive decline in murine models of AD
90 overexpressing mutated human APP and presenilin 1 linked to familial AD (17, 20, 21).
91 Inasmuch as PPARs expression is modified in AD brains (22), we hypothesized that the
92 function of PPAR α could be impaired in AD and may therefore contribute to the progression
93 of the disease.

94 In this study, we report that *PPARA* mRNA level and the expression of PPAR α related target
95 genes are modified in brains from LOAD and EOAD cases with a rare *APP* duplication and
96 that *PPARA* expression inversely correlated with the expression of human APP (hAPP) protein
97 in AD. We previously demonstrated that increased expression of hAPP in cortical cells inhibits
98 both cholesterol turnover and FA biosynthesis needed for neuronal network activity (23). In
99 addition, we observed that PPAR α deficiency leads to decreased LTP as well (17). Therefore,
100 we have investigated whether modification in *PPARA* expression could be mediated by APP
101 expression levels. We report that *PPARA* mRNA and expression of related PPAR α downstream
102 target genes are decreased in transgenic mice and in cultured cortical cells overexpressing non-
103 mutated human APP, while opposite results were observed in APP silenced cortical networks.
104 Moreover, APP-mediated effects on *PPARA* expression and thereby on synaptic activity were
105 reversed with PPAR α specific modulators in cultured cortical cells.

106 **Results**

107

108 **Human APP-dependent expression and i of PPAR α in brains from patients with late-onset**
109 **Alzheimer disease and in early-onset cases with a duplication of the *APP* locus.**

110 We first analysed the expression of *PPARA* mRNA level in human post-mortem brains from
111 controls and late-onset AD cases (LOAD) (**Supplemental Table 1**). A 3-fold increase in the
112 relative expression of *PPARA* (2.88 ± 0.63) was observed in the frontal cortex of LOAD
113 compared to non-demented control samples (**Figure 1A**). We next analysed the activation of
114 PPAR α in control and LOAD samples by measuring mRNA level of *ACOX1*, the first identified
115 target gene of PPAR α that encodes Acyl-CoA Oxidase 1, a rate-limiting enzymes involved in
116 peroxisomal FA oxidation (11). A 5-fold increase in the relative expression of *ACOX1* ($4.95 \pm$
117 1.07) gene was measured in the frontal cortex of LOAD samples compared to controls (**Figure**
118 **1B**). The huge variability in the increased expressions of *PPARA* and *ACOX1* measured in AD
119 brains prompted us to analyse a possible correlation between *PPARA* and *ACOX1* mRNA
120 expressions in LOAD. We observed a strong correlation between PPAR α expression (*PPARA*
121 mRNA) and activation (*ACOX1* expression) in LOAD (**Figure 1C**). Moreover, we observed
122 that the *CPT1A* (4.97 ± 1.37) gene encoding Carnitine Palmitoyltransferase 1A, a rate-limiting
123 enzymes involved in mitochondrial FA oxidation (11), and *PDK4* (3.83 ± 0.81) encoding
124 Pyruvate Dehydrogenase Kinase 4, which regulates the rate-limiting step of glucose oxidation
125 by switching off the pyruvate dehydrogenase complex (24), were also increased in the frontal
126 cortex of LOAD compared to non-demented control samples (**Supplemental Figure 1A**), two
127 non-specific PPAR α genes known to be nevertheless regulated by PPAR α (11). Inasmuch as
128 *ACOX1*, *CPT1A* and *PDK4* expressions are related to FA and glucose oxidation, these results
129 corroborate abnormalities in brain FA and glucose metabolism, bioenergetics, and
130 mitochondrial function reported in AD (12, 13, 25). Since lipid biochemistry is disrupted in AD

131 (10, 26) and given that one of the main neuropathological characteristics involved in AD
132 pathogenesis implies the APP protein (27, 28), which we have previously reported to decrease
133 both cholesterol and FA biosynthesis when its expression level increases (23), we wondered
134 whether modifications in *PPARA* expression observed could be related to human APP (hAPP)
135 expression. While the global expression level of full-length hAPP protein was unchanged in
136 LOAD compared to controls (**Figures 1D** and **1E**), a case by case analysis reveals a tight inverse
137 correlation between hAPP protein and *PPARA* expressions in LOAD, but not in control brains
138 (**Figures 1F** and **1G**), suggesting that *PPARA* expression is regulated by hAPP expression level
139 only in LOAD. From these results, we next analysed *PPARA* and PPAR α downstream target
140 genes expressions in human brains samples from rare early-onset AD (EOAD) cases with a
141 microduplication in the *APP* locus (**Supplemental Table 2**) (27, 29). *PPARA*, *ACOX1*, *CPT1A*
142 and *PDK4* mRNA levels were 3 to 4-fold decreased (0.35 ± 0.15 , 0.22 ± 0.09 , 0.37 ± 0.10 , 0.22
143 ± 0.15 , respectively) (**Figures 1H**, **1I** and **Supplemental Figure 1B**) in EOAD cases compared
144 to controls, in whom a two-fold increase in brain hAPP protein expression (2.13 ± 0.25) was
145 observed compared to age-matched controls (**Figures 1J** and **1K**), supporting therefore that
146 increase in hAPP expression was concomitant with decrease in *PPARA*. Altogether these results
147 suggest that non-mutated hAPP expression is inversely correlated with the expression of
148 *PPARA* and PPAR α target genes both in LOAD and EOAD cases, but not in control human
149 brains.

150

151 **Brain *Ppara* expression and its downstream target genes are decreased in transgenic mice**
152 **overexpressing wildtype human APP.**

153 Among transgenic mouse models created to gain insight into AD pathology, the most
154 commonly used are those overexpressing mutated hAPP linked to familial AD (30) resulting in
155 the formation of brain amyloid plaques, one of the pathological hallmarks observed in the brain

156 of AD patients. Because of their intrinsic relationship, the impact of hAPP expression on *Ppara*
157 expression was separated from that of amyloid deposition by studying the hemizygous
158 transgenic mouse model overexpressing wildtype form of hAPP (hAPP_{WT} formerly known as
159 line I5 mouse strain (31)), a mouse model displaying spatial learning and memory deficits with
160 high cortical level of hAPP and no evidence for A β deposition (31, 32). By western blot analysis
161 with an antibody that recognizes human and mouse APP, 2 to 3-fold higher APP levels were
162 observed in hAPP_{WT} as compared to WT mice at early (3-4 months old: 2.67 ± 0.34), advanced
163 (6-8 months old: 1.86 ± 0.21) and late ages (11-12 months old: 2.63 ± 0.30) (**Figure 2A** and
164 **2B**) as expected (32). A trend of a higher expression of brain *Ppara* was observed together with
165 a trend of increased *Acox1*, *Cpt1a* and *Pdk4* mRNA levels along with age in WT mice (**Figures**
166 **2C - 2F**), indicating that the aged brain retains enhanced FA utilization compared to young WT
167 mice, meaning that aging brain could switch to FA oxidation (33, 34). While a similar profile
168 was observed in hAPP_{WT} mice at early and advanced ages, a 2 to 5-fold decrease in *Ppara*,
169 *Acox1*, *Cpt1a* and *Pdk4* mRNA levels was observed (0.46 ± 0.04 , 0.58 ± 0.06 , 0.50 ± 0.10 , 0.91
170 ± 0.06 , respectively) in 11-12 months old hAPP_{WT} mice compared to WT littermates at the same
171 age (**Figures 2C - 2F**), an age at which severe cognitive deficits are detected (32, 35). Metabolic
172 alterations including deficits for acylcarnitines have previously been reported in brain of a
173 transgenic mouse model of AD bearing mutated APP and PS1 transgenes, in which early brain
174 amyloid deposition and cognitive impairment occur (36). Nevertheless, our results indicate that
175 in absence of amyloid deposition, non-mutated hAPP overexpression is sufficient to induce a
176 decrease in brain *Ppara* expression and its downstream target genes and suggest therefore that
177 activation of β -oxidation pathways of FA in the mitochondria might be perturbed in the brain
178 of APP_{WT} mice. Moreover, besides hAPP overexpression, an additional age-dependent
179 contribution is needed to observe a decrease in the expression of PPAR α downstream target

180 genes, a decrease similar to that previously observed in human brain samples with *APP*
181 duplication.

182

183 **Wy14643 PPAR α agonist prevents human APP-induced decreases in PPAR α activation**
184 **and synaptic activity in cortical cultures.**

185 The finding that activation of all PPARs, but especially PPAR γ , has salutary effects on
186 neurodegenerative disorders including AD (19) and that a promising role of PPAR α in AD
187 therapy emerged (10, 37), we wondered whether PPAR α specific agonist could interfere with
188 hAPP-mediated decrease in PPAR α target genes expression observed. To address this question,
189 we expressed neuronal wild-type hAPP isoform in cultured rat cortical cells. Full-length hAPP
190 expression was achieved by transducing primary cortical cultures with a recombinant
191 adenoviral vector at 6 DIV and hAPP expression was probed by immunoblotting at 13-14 DIV
192 with the hAPP specific WO2 antibody (**Figure 3A**). We have previously shown that transgene
193 expression was homogeneous, did not affect cell density and viability and remained stable over
194 time (38). By using an antibody that recognizes both human and endogenous rat APP, a nearly
195 2-fold increase in total APP levels (1.87 ± 0.15) was observed compared to control cells
196 transduced with an adenovirus encoding the human recombinant green fluorescent protein
197 (hrGFP) (**Figure 3A** and **3B**). As previously observed in human and mouse brain lysates
198 overexpressing hAPP protein, *Ppara* (0.49 ± 0.05), *Acox1* (0.40 ± 0.06), *Cpt1a* (0.39 ± 0.06)
199 and *Pdk4* (0.46 ± 0.10) mRNA levels were reduced by about 60 % in hAPP expressing cells
200 compared to hrGFP vehicle treated controls (**Figure 3C** and **3D**). It is very well known that
201 cancers reprogram their metabolism to adapt to environmental changes. *Cpt1a* fuels lipid beta-
202 oxidation by producing acyl-carnitines in the mitochondria (39). It was recently demonstrated
203 that in prostate cancer cell models, overexpression of *Cpt1a* is associated with a significant
204 increase in intracellular lipase activity (40), a step which liberates fatty acids from triglyceride

205 stores which can then be used for β -oxidation (41). Consequently, overexpression of *Cpt1a*
206 increases free fatty acid (FFA) content in these cancer cells. We measured whether modification
207 in *Cpt1a* expression influences FFA content in our cultured cortical cells. In hAPP expressing
208 cells, a decrease in *Cpt1a* expression was concomitant with a 70 % decrease in cell FFA content
209 (0.32 ± 0.06) compared to hrGFP control (**Supplemental Figure 2A**), demonstrating that
210 modification in *Cpt1a* expression affects fatty acids metabolism in our cortical cells in culture.
211 Moreover, since *Pdk4* is known to play a role in the metabolic switch from glycolysis to
212 mitochondrial oxidative phosphorylation (OXPHOS) (24), decrease in *Pdk4* observed indicates
213 that hAPP expression enhances glycolysis in cortical cells (42). Cells were then treated with
214 pirinixic acid (Wy14643), a synthetic PPAR α agonist (reviewed in (19, 43)). As expected, the
215 basal expression of *Acox1* (1.66 ± 0.16), *Cpt1a* (1.72 ± 0.21), and *Pdk4* (1.61 ± 0.16) genes
216 were increased in Wy14643 treated hrGFP cells compared to vehicle treated cells (**Figure 3D**).
217 Moreover, Wy14643 was able to inhibit the hAPP-mediated decrease in *Acox1*, *Cpt1a*, and
218 *Pdk4* mRNA levels (**Figure 3D**), indicating that the pharmacological modulation of PPAR α is
219 able to restore hAPP-mediated effects on PPAR α target genes expression in cortical cells in
220 culture.

221 As PPAR α deficiency affects neuronal activity in cultured hippocampal neurons (16) and
222 synaptic plasticity in mice (17), we hypothesized that decrease in PPAR α target genes
223 expression could contribute to the hAPP-mediated synaptic transmission silencing of cortical
224 networks (23, 44, 45). To study the effect of 5-7 days hAPP expression on synaptic activity, we
225 performed whole-cell voltage clamp recordings. Resting membrane potential (RMP) was more
226 negative ($\Delta V_m -8.04 \text{ mV} \pm -1.16$) (38) (**Figure 3E**) and concomitant decreases in spontaneous
227 total synaptic activity (**Figure 3F**) frequency (hrGFP, $1.50 \pm 0.37 \text{ Hz}$; hAPP, $0.21 \pm 0.06 \text{ Hz}$;
228 **Figure 3G**) and amplitude averages (hrGFP, $32.41 \pm 1.30 \text{ pA}$; hAPP, $20.93 \pm 1.22 \text{ pA}$, **Figure**
229 **3H**) were measured in hAPP neurons compared to hrGFP controls. However, Wy14643

230 treatment partially prevented the effect of hAPP expression on synaptic activity (**Figure 3F**),
231 restored RMP and increased both frequency (vehicle hAPP, 0.21 ± 0.06 Hz; Wy14643 hAPP,
232 2.58 ± 0.51 Hz) and amplitude of synaptic events (vehicle hAPP, 20.93 ± 1.22 pA; Wy14643
233 hAPP, 27.79 ± 0.67 pA), while no significant changes were observed in Wy14643 hrGFP
234 compared to vehicle treated controls (**Figures 3E, G and H**). Altogether, these results indicate
235 that PPAR α activation with a specific agonist can prevent hAPP-mediated synaptic activity
236 depression of cortical networks.

237

238 **GW6471 PPAR α antagonist inhibits APP knockdown-induced increases in PPAR** 239 **activation and synaptic activity in cortical cultures.**

240 To further investigate the possible modulation of PPAR α activation by APP, APP expression
241 was reduced in cortical cells by using shRNA construct designed to target endogenous APP
242 (shAPP). The knockdown of endogenous rat APP was achieved by transducing cells on 6 DIV
243 with recombinant lentiviruses encoding shAPP and a scrambled shRNA encoding GFP (shScra-
244 GFP) was used as a negative control. At 13-14 DIV, blots were probed with an antibody that
245 recognizes the 19 carboxyl-terminal amino acids of endogenous APP (**Figure 4A**). As expected,
246 a 66.66 ± 5.7 % reduction of endogenous APP expression (38) (**Figure 4B**) with no induction
247 in the expression of APLP1 and APLP2 for functional compensation for the loss of APP were
248 observed as we have previously reported (23, 38). Unlike hAPP cells, APP knockdown induced
249 a 2-fold increase in *Ppara* (1.89 ± 0.26), *Acox1* (2.19 ± 0.24) and *Cpt1a* (1.98 ± 0.18) and
250 robustly increased *Pdk4* (4.22 ± 0.63) mRNA levels compared to controls (**Figure 4C and 4D**),
251 indicating that PPAR α activation is increased in these cells. Contrary to hAPP expressing cells,
252 an increase in *Cpt1a* expression was concomitant with a 75% increase in FFA content ($1.75 \pm$
253 0.10) in shAPP cells compared to shScra-GFP control cells (**Supplemental Figure 2B**). These
254 results confirm that APP-mediated modification in *Cpt1a* expression affects fatty acids

255 metabolism in cortical cells. Moreover, these results suggest that reduction in endogenous APP
256 enhances the transport of FAs into the mitochondria for β -oxidation and that shAPP cells may
257 be less glycolytic (46). We next used GW6471 to specifically inhibit PPAR α activity (47) in
258 order to counteract the shAPP-mediated effect on PPAR α activation. The effectiveness of
259 GW6471 was confirmed by the decreased expression of *Cpt1a* observed in both treated shAPP
260 (0.69 ± 0.18) and shScra-GFP (0.41 ± 0.06) cells compared to vehicle-treated controls (**Figure**
261 **4C**), while no changes were observed in *Acox1* and *Pdk4* mRNA levels. These results indicate
262 that the GW6471 PPAR α antagonist partially inhibits APP knockdown-induced increase in
263 PPAR α activation and specifically affects *Cpt1a* expression in cortical cells.

264 To address whether increase in PPAR α activation could contribute to shAPP-mediated increase
265 in neuronal activity of cortical networks as reported (23), we performed whole-cell voltage
266 clamp recordings in APP knocked down neurons and treated them with GW6471. RMP was
267 more positive ($\Delta V_m -11.20 \text{ mV} \pm -0.22$) (**Figure 4E**) and concomitant increase in total
268 synaptic activity (**Figure 4F**) frequency (shScra-GFP, 1.30 ± 0.06 Hz; shAPP, 2.55 ± 0.27 Hz;
269 **Figure 4G**), with no significant change in the amplitude (shScra-GFP, 51.89 ± 10.49 pA;
270 shAPP, 51.42 ± 3.09 pA, **Figure 4H**), was measured in shAPP compared to shScra-GFP
271 controls. Moreover, GW6471 restored RMP, frequency and amplitude in treated shAPP to
272 levels similar to vehicle treated controls (**Figures 4E-H**). Altogether, these results indicate that
273 APP expression levels modulate the activation of PPAR α and thereby synaptic function and
274 that pharmacological approaches targeting PPAR α allow to reverse APP mediated effects
275 observed in cortical cells in culture.

276

277 **Control of synaptic activity by APP disappears in the absence of PPAR α in cortical**
278 **cultures.**

279 To address whether APP-mediated control of synaptic activity could be PPAR α dependent,
280 primary cultures of cortical cells derived from WT and PPAR α deficient (*Ppara*^{-/-}) mice
281 (**Figure 5A**) were transduced with recombinant viruses in order to express hAPP (**Figure 5B**)
282 or to repress endogenous APP (**Figure 5C**). With a similar extent as observed previously in rat
283 primary cultures, a two fold increase (2.22 ± 0.25) and a 60 % reduction (0.40 ± 0.02) in total
284 APP levels were observed in hAPP and shAPP WT relative to infected WT controls. Moreover,
285 PPAR α deficiency did not affect total APP content increase (2.24 ± 0.22) and decrease ($0.45 \pm$
286 0.05) observed in hAPP and shAPP *Ppara*^{-/-} compared to hAPP and shAPP WT, respectively
287 (**Figure 5D**). Although the knockout of PPAR α increased averages of total synaptic activity
288 frequency (4.34 ± 0.51 Hz) and amplitude (64.47 ± 3.45 pA) in all infected conditions, PPAR α
289 deficiency totally prevented APP-mediated effects on RMPs, synaptic events frequencies and
290 amplitudes recorded in hAPP and shAPP *Ppara*^{-/-} compared respectively to hrGFP and shScra-
291 GFP controls (**Figures 5E-H**). Altogether, these results suggest that PPAR α is a downstream
292 mediator of APP-mediated control on synaptic activity.

293

294 **Discussion**

295

296 We report here that *PPARA* expression and PPAR α downstream target genes are inversely
297 correlated with hAPP expression in both LOAD and EOAD with a microduplication of the *APP*
298 locus. Such an effect of hAPP expression was also observed in hAPP transgenic mice and in
299 cortical networks, in which pharmacological approaches targeting PPAR α alleviate APP-
300 mediated synaptic dysfunction.

301 The overall increase in the expression of *PPARA mRNA* that we have observed in LOAD is not
302 in agreement with previous results reporting globally reduced expression level of PPAR α in
303 AD brains (22). However, a case by case analysis reveals a tight inverse correlation between
304 hAPP protein and *PPARA* expressions in our LOAD samples, but not in control brains,
305 suggesting that *PPARA* expression is regulated by hAPP expression level only in LOAD. The
306 large variability of both hAPP protein and *PPARA mRNA* contents observed in the LOAD
307 group could probably account in part for the discrepancy with the results published by de la
308 Monte and colleagues (22). Expression, trafficking and processing of APP are regulated in a
309 complex way including prominent changes during pathological states. It was previously
310 reported that APP expression is upregulated under conditions of metabolic stress (48), ischemia
311 (49), brain injury (50) and inflammation (51) and that individual APP expression is
312 heterogeneous in AD patients (49). Moreover, our results put forward that APP expression
313 seems to play a determining role on *PPARA* expression in LOAD, but not in controls, in which
314 no correlation between hAPP and *PPARA mRNA* contents was observed. Furthermore, our
315 results demonstrate that in addition to *PPARA* gene expression, expression of *ACOX1*, *CPT1A*
316 and *PDK4* PPAR α target genes, are inversely correlated with hAPP expression when LAOD
317 samples are analysed individually. This inverse correlation between hAPP and *PPARA*
318 expression and activation is confirmed in EOAD cases with a rare duplication of the *APP* locus.

319 We conclude that particular attention should be paid to the level of hAPP expression in each
320 AD case studied when the expression of *PPARA* is considered. Such an inverse correlation
321 between hAPP and *PPARA* expression was not observed in control brains, indicating a specific
322 function of hAPP in AD.

323 In the brain of AD patients, microglial activation is observed in the vicinity of senile plaques at
324 all stages of the disease and is accompanied by increased levels of pro-inflammatory molecules
325 (*e.g.* TNF, IL-1 β , IL-6, prostaglandins) (52). Genome-wide association studies identified
326 inflammation-related genes as potential risk factors for developing AD (53). In addition, it was
327 recently reported that APP expression is increased under inflammatory processes in an AD
328 transgenic mouse model (51). Therefore, we cannot exclude that inflammation could mediate
329 changes in brain APP expression that could thereby affect *PPARA* expression in AD samples
330 analysed.

331
332 Increases in *ACOX1* and *CPT1A* observed in LOAD with a low hAPP content indicate that β -
333 oxidation pathways of very long chain FA in the peroxisome and short-, medium-, and long-
334 chain fatty acids in the mitochondria are activated. Activation of FA oxidation might take place
335 to compensate for compromised pyruvate dehydrogenase complex (PDC) to provide alternative
336 sources of acetyl-CoA to sustain ATP energy supply. Indeed, a concomitant increase in the
337 expression of *PDK4* that catalyses the phosphorylation-dependent inactivation of the
338 mitochondrial PDC (24) was observed in LOAD, in whom a reduction in PDC activity was
339 previously reported (54). As mitochondrial PDC connects glycolysis to oxidative metabolism
340 (55) and as PDK4 up-regulation facilitates FA oxidation, in particular when glucose is scarce
341 during energy deprivation (56), *PDK4* increase observed in LOAD brain correlates with the
342 reduced cerebral glucose utilization found in AD patients (12), in which early brain peroxisomal
343 and mitochondrial function deficits have been reported (reviewed in (22, 57)). Although a shift

344 in brain metabolism from glucose-driven energy supply to a ketogenic/FA oxidation pathways
345 is reported in LOAD (58), this shift could depend on the level of APP expression. In addition,
346 an opposite shift may take place in EOAD carrying a microduplication of the *APP* locus (27,
347 29). Indeed, an inverse correlation was observed in brain samples from *APP*dup cases, in which
348 increase in hAPP is concomitant with decreases in *PAPARA*, *ACOX1*, *CPT1A* and *PDK4*
349 expression. We conclude that metabolic shifts observed in LOAD and EOAD could rely on
350 hAPP expression level, suggesting that hAPP by controlling *PPARA* expression and its
351 downstream target genes might be considered as an essential metabolic mediator in AD, but not
352 in control brains. Although modifications in brain *PAPARA*, *ACOX1*, *CPT1A* and *PDK4*
353 expression observed could be mediated by variations in hAPP expression in AD, a role for
354 hAPP cleavage products including A β , tau phosphorylation, brain inflammation, synaptic loss
355 and amyloid burden reported in AD brains cannot be ruled out (2).

356 Interestingly, neuropathological changes observed in AD were reported in patients with Down
357 syndrome (DS), in whom the presence of an extra chromosome 21 leads to intellectual
358 disability. Association between AD and DS is partially due to the overexpression of hAPP that
359 results from the location of *APP* gene on chromosome 21 (59). Moreover, mitochondrial
360 deficits, increase in oxidative stress, impaired glucose and lipid metabolism leading to a reduced
361 rate of energy metabolism were reported in DS (reviewed in (60)). Recently, severe brain
362 malformations with pyruvate dehydrogenase deficiency and DS were reported (61) and the
363 Down syndrome critical region 2 protein was shown to inhibit the transcriptional activity of
364 PPAR β in cell line, indicating a potential dysfunction of PPAR activation in DS, in which hAPP
365 expression level is increased (62).

366

367 APP-dependent modulation of brain *PPARA*, *ACOX1*, *CPT1A* and *PDK4* expression was not
368 only observed in human AD brain but also in mice. Indeed, we show that overall increase in

369 APP expression lowers brain *Ppara* expression and thereby *Acox1*, *Cpt1* and *Pdk4* in hAPP_{WT}
370 mice at late stages (31, 32). An increase in *Acox1* expression was found in the hippocampus of
371 young Tg2576 mice, a mouse model of AD harbouring the human Swedish familial AD
372 mutation that develops parenchymal amyloid plaques at 11-13 months of age, while *Acox1*
373 expression was found to be decreased in old animals (63, 64). Moreover, *Pdk4* decrease
374 observed in old hAPP_{WT} mice corroborates the decrease in the PDC reported in brain
375 synaptosomes of Tg2576 mice (65). However, decreases in *Acox1* and *Pdk4* observed in APP_{WT}
376 mice rule out a possible involvement of amyloid plaques in these mice, which are devoid of
377 brain A β deposition (31, 32).

378

379 APP-dependent regulation of *Ppara*, *Acox1*, *Cpt1a* and *Pdk4* mRNA observed in hAPP_{WT} mice,
380 EOAD with a duplication of the *APP* locus and LOAD cases were recapitulated in hAPP
381 expressing and silenced APP cultured cortical cells, indicating a critical involvement of APP
382 expression in the regulation of *Ppara* and its downstream target genes. The diminution of *Pdk4*
383 observed in hAPP expressing cells indicates that hAPP expression and/or increase in total APP
384 content enhances glycolytic metabolism, as reported in human neuroblastoma cells in which
385 increase in neuronal hAPP levels mediates an A β -independent *Pdk4* downregulation (42).
386 Conversely, the robust *Pdk4* increase observed in APP-silenced cortical cells suggests that APP
387 reduction lowers cell glycolytic capacity (46). Variations in APP expression therefore modulate
388 *Ppara* expression and its downstream target genes in cultured cortical cells, strengthening a
389 potential role of APP expression as metabolic mediator. Moreover, a pivotal role of Pdk4 and
390 metabolic flexibility was reported in the brain that utilizes glucose as primary energy source
391 (24). Astrocytes expressed more Pdk4 than neurons and have lower PDC activity (66),
392 indicating that APP-mediated changes in *Pdk4* expression might occur primarily in astrocytes
393 in our cultured cells. Moreover, increase in *Cpt1a* observed in APP knocked down cells takes

394 place also probably in astrocytes (33), in which FA oxidation predominantly occurs to
395 contribute up to 20% of the total brain energy requirement as reported in brain primary cultures
396 (67). Given that there is a tight metabolic coupling between astrocytes and neurons, a metabolic
397 transition from glycolysis to OXPHOS could occur in APP knocked down cells to provide
398 adequate ATP level to meet the increased energy demand needed for the sustained synaptic
399 activity observed.

400 While we observed a depressive effect of hAPP expression on synaptic transmission that could
401 result from an A β -dependent postsynaptic silencing of α -amino-3-hydroxy-5-methyl-4-
402 isoxazolepropionic acid (AMPA) (45) and N-methyl-D-aspartate (NMDA) receptor-mediated
403 currents (44), synaptic excitatory transmission increased in APP-silenced neurons suggests that
404 changes in neuronal activity drive changes in metabolic flux or vice versa. While energy
405 metabolism of neurons is mainly aerobic and that of astrocytes mainly anaerobic glycolysis,
406 OXPHOS was shown to be the main mechanism initially providing energy to power neuronal
407 activity (68). Accordingly, miniature excitatory postsynaptic currents frequency was shown to
408 be increased in neurons derived from APP knock-out mice (69), in which a resistance to a high
409 fat diet (HFD)-induced obesity was observed and linked to higher energy expenditure and lipid
410 oxidation (70). Moreover, changes in synaptic activity observed could be mediated by the Cpt1c
411 isoform. Indeed, despite the inability of the brain specific Cpt1c isoform to β -oxidize long chain
412 FAs contrary to Cpt1a (71), Cpt1c could enhance whole-cell currents of shAPP neurons by
413 increasing the trafficking and the surface expression of the GluA1 subunit containing AMPA
414 receptors to enhance AMPA receptors mediated currents (71).

415

416 Our findings also put forward that APP-mediated changes in the expression of *Acox1*, *Cpt1a*
417 and *Pdk4* are driven by metabolic regulators and in particular PPAR α . The central role of
418 PPAR α in FA catabolism is very well known (11). PPAR α increases expression of genes

419 encoding peroxysomal and mitochondrial enzymes including *Acox1* and *Cpt1* and both PPAR α
420 and PPAR- β/δ but not PPAR- γ also activate the *Pdk4* encoding gene (11). We report that
421 PPAR α modulators are able to reverse APP mediated effects observed in cultured cortical cells.
422 PPAR α synthetic agonist Wy14643 normalizes the expression of PPAR α target genes and
423 restores synaptic activity depressed in hAPP expressing cells. This could result from the
424 proliferation of peroxisomes and/or the expression of peroxisomal enzymes that prevents A β -
425 mediated cell death and/or oxidative stress as reported in rat hippocampal and cortical cultures,
426 respectively (72, 73). Moreover, PPAR α agonists have been reported to promote the non-
427 amyloidogenic processing of APP in hippocampal neurons by enhancing the expression of the
428 α -secretase ADAM10 that precludes A β generation from APP and increases the release of the
429 soluble APP α fragment (74). Therefore, PPAR α agonist Wy14643 could promote the
430 nonamyloidogenic processing of APP alleviating therefore the A β -mediated negative feedback
431 on synaptic transmission observed in hAPP neurons.

432 PPAR α plays a key role in inflammation and PPAR agonists are anti-inflammatory drugs
433 targeting microglia and astrocytes (11). However, activation of PPAR α also produces a strong
434 neuronal signature, by regulating glutamatergic and cholinergic mediated dopaminergic
435 transmission in the brain (75). Although our cortical cells in culture contain both neurons and
436 astrocytes, patch clamp analyses were performed exclusively on neurons, confirming that
437 modulation of the activity of PPAR α influences neuronal activity.

438 Furthermore, we report that PPAR α antagonist GW6471 inhibits APP knockdown-induced
439 increases in PPAR activation and synaptic activity in cortical cultures. GW6471 decreases the
440 expression of upregulated *Cpt1a* without modifying the expression of *Acox1* and *Pdk4* of
441 shAPP cells, pointing therefore to differences between Wy14643 and GW6471 in their binding
442 affinity and/or in the recruitment of PPAR α nuclear co-activators and/or -repressors (47).
443 However, we report that GW6471 is able to normalize intensive synaptic activity of shAPP

444 cells. The knock-down of APP in neuronal precursor cells of the hippocampus was previously
445 reported to affect synaptic GluN2B-containing NMDA receptors (76) and PPAR α , but not
446 PPAR β and PPAR γ was shown to regulate cyclic AMP response element binding and therefore
447 hippocampal plasticity-related genes encoding GluN2A/2B and GluA1 subunits of NMDA and
448 AMPA receptors (16, 17). From these observations, GW6471 could then affect both GluN2B
449 and GluA1 expressions and/or Cpt1c-mediated trafficking of GluA1 (71) to modulate synaptic
450 activity of shAPP neurons. Furthermore, we report that deficiency of PPAR α in cortical cells
451 abrogates APP-mediated controls of synaptic activity, confirming that PPAR α is an APP-
452 downstream mediator.

453

454 A growing body of evidence suggests that synaptic dysfunction may occur long before synapse
455 loss in early AD and may therefore contribute to cognitive dysfunction (3). Abnormalities in
456 brain activity have been reported in both LOAD and EOAD (reviewed in (77)), in which an
457 increased incidence of seizures has been observed, and greater risk for seizures were previously
458 recorded in patients with *APP* duplication and in DS with dementia (78, 79). Spontaneous
459 seizures and sharp wave discharges have been observed in several transgenic models of AD
460 expressing APP mutated or not (32). Moreover, APP overexpression, but not a subsequent A β
461 increase, leads to hypersynchronous network activity in an APP transgenic mouse model of
462 AD, suggesting that APP overexpression elicited network alterations through an indirect
463 mechanism (80). Although salutary effects of PPAR α and γ agonists on memory have been
464 reported in several preclinical AD models that overexpress APP, human clinical trials using
465 PPAR γ agonists in the treatment of AD are less encouraging (reviewed in (10, 37)). A U-shaped
466 relationship between APP level and its functions has been put forward given that both mice
467 overexpressing or lacking APP exhibit, *inter alia*, age-dependent deficits in long-term

468 potentiation, an activity-dependent enhancement of synaptic strength involved in memory
469 processing (18), learning, vulnerability to seizures and metabolic stress (reviewed in (77)).

470

471 As cell energy metabolism and synaptic activity are closely related, it is still questionable
472 whether a PPAR α agonist or antagonist could help for synaptic abnormalities associated to
473 cognitive impairments observed in AD. However, our results put forward that the expression
474 of APP as a metabolic regulator should be considered throughout the course of the disease, in
475 which potential APP-mediated metabolic switches driven by PPAR α could occur. Moreover,
476 overlapping metabolic dysfunctions reported in AD and metabolic diseases such as obesity and
477 type 2 diabetes (for review see (10)) that have been identified as AD risk factors, emphasize an
478 essential role of lipid and glucose metabolism in the etiology of AD. Therefore,
479 pharmacological modulation of the PPAR α metabolic regulator could be part of a personalized
480 multi therapy that could help AD patients, in function of their level of APP expression.

481

482

483

484 **Methods**

485

486 For cell culture, semiquantitative RT-PCR, immunoblotting analysis, recombinant viruses and
487 cell transduction, an extended section is provided in Supplemental Methods.

488

489 **Human tissues and animals**

490 **Human tissues.** Frontal cortex samples from 10 human control subjects and 11 demented
491 patients were analysed. All patients were clinically diagnosed. Neuropathological examinations
492 were performed on multiple formalin fixed, paraffin embedded postmortem frozen brain tissues
493 and confirmed clinically diagnosed patients as late-onset AD cases. Genetic analyses were
494 performed on early-onset AD patients with *APP* microduplication mapping to chromosome
495 21q2.1, including the *APP* locus with no contiguous gene. An overview of the donor
496 information and postmortem variables is summarized in Supplemental Tables 1 and 2.

497 **Animals.** Pregnant Wistar rats were obtained from the UCLouvain animal facility (Brussels,
498 Belgium) and P0-P1 pups from *PPAR α* deficient (*Ppara*^{-/-}) mice (JAX stock #008154) were
499 utilised (81) for embryonic rat and mouse cortical cell cultures, respectively. Age-matched non-
500 transgenic wild type littermates were used as controls. For *Ppara*^{-/-} mice, genotypes were
501 confirmed by PCR amplification from mouse tail biopsies DNA using KAPA Express Extract
502 combined with KAPA2G Robust HotStart Ready Mix (Sopachem, Belgium, #KK7152) by
503 using the following standard Jackson Labs suggested primers (see Supplemental Table 3).

504 3-4, 6-8 and 11-12 months old transgenic male mice expressing a transgene containing wildtype
505 human APP (APPWT line I5 mouse strain (31) JAX stock #004662) were used. Genotypes
506 were confirmed by PCR amplification with the following standard Jackson Labs suggested
507 primers (see Supplemental Table 3). Mice were group-housed under standardized conditions
508 (12/12 h dark/light cycle, not reversed), with free access to food (SAFE A03, SAFE Diets) and

509 water *ad libitum*. Temperature in the vivarium was maintained between 20 and 24°C, and
510 humidity between 45 and 65%.

511 **Brain mouse tissue collection.** Brains from transgenic mice were snap frozen in liquid nitrogen
512 and stored at –80°C until further use (RNA isolation for RT-qPCR and Western blotting).

513

514 **Reagents and antibodies.** When unmentioned, reagents for cell culture and western blotting
515 were purchased from Thermo Fisher Scientific. Antibodies were purchased as indicated in
516 Supplemental Table 4.

517

518 **Treatments.** At 13-14 DIV, cells were treated for 24 h with 10 µM Wy14643 [[4-Chloro-6-
519 [(2,3-dimethylphenyl)amino]-2-pyrimidinyl]thio]acetic acid (Tocris, #1312), 5µM GW6471
520 N-((2S)-2-(((1Z)-1-Methyl-3-oxo-3-(4-(trifluoromethyl)phenyl)prop-1-enyl)amino)-3-(4-(2-
521 (5-methyl-2-phenyl-1,3-oxazol-4-yl)ethoxy)phenyl)propyl)propanamide (Tocris, #4618) or
522 vehicle (0.0001% and 0.005% DMSO, respectively). For electrophysiology, cells were treated
523 with 1µM GW6471.

524

525 **RNA extraction and Real-time PCR.** Total RNA was isolated by TriPure Isolation Reagent
526 (Roche, #11667165001) according to the manufacturer's protocol. RNA samples were
527 resuspended in DEPC-treated water (1µg/10µL). Reverse transcription was carried out with the
528 iScript cDNA synthesis Kit (Bio-Rad Laboratories, #1708891) using 1 µg of total RNA in a
529 total volume reaction of 20 µL. Real-time PCR was performed for the amplification of cDNAs
530 with specific primers (Sigma-Aldrich, see Supplemental Table 5). Real-time PCR was carried
531 out in a total volume of 25 µL containing 16 ng cDNA template, 0.3 µM of the appropriate
532 primers and the IQTM SYBR® Green Supermix 1x (Bio-Rad Laboratories, #1708885). The
533 PCR protocol consisted of 40 amplification cycles (95°C for 30 s, 60°C for 45 s and 79°C for

534 15 s) and was performed using an iCycler IQ™ multicolor Real-Time PCR detection system
535 (Bio-Rad Laboratories), used to determine the threshold cycle (Ct). Melting curves were
536 performed to detect nonspecific amplification products. A standard curve was established for
537 each target gene using four-fold serial dilutions (from 100 to 0.097 ng) of a cDNA template
538 mix prepared in the same conditions. Each sample was normalized to relative expression level
539 of ribosomal protein L32 (*Rpl32*). Calculation of Ct, standard curve preparation and
540 quantification of mRNAs in each sample were performed using the "post run data analysis"
541 software provided with the iCycler system (Bio-Rad).

542

543 **Free fatty acid measurement.** Cells in culture ($4 \cdot 10^5$ cells / cm²) were analysed at 13-14 DIV.
544 Total lipids were extracted according to manufacturer guidelines (Free Fatty Acid
545 Quantification Kit, #ab65341, Abcam). Briefly, fatty acids were converted to their CoA
546 derivatives and subsequently oxidized with concomitant generation of color. Octanoate and
547 longer fatty acids were quantified by colorimetric (spectrophotometry at = 570 nm) with
548 detection limit 2 μM free fatty acid in samples. Relative free fatty acids were quantified based
549 on the protein content.

550

551 **Electrophysiology.** Cells in culture ($8 \cdot 10^4$ cells / cm²) were analysed at 13-17 DIV. Total
552 synaptic activity was recorded in voltage-clamp mode (holding potential -60mV). The
553 recording bath solution contained 150 mM NaCl, 5.4 mM KCl, 2 mM CaCl₂, 2.1 mM MgCl₂,
554 10 mM HEPES, 10 mM Glucose (pH adjusted to 7.4 with NaOH, osmolarity: 320 mOsm/l at
555 room temperature). Borosilicate glass capillaries were pulled using a P97 horizontal puller
556 (Sutter Instruments) and had a resistance of 4-8 MΩ when filled with the internal solution. The
557 internal pipette solution contained 140 mM KCl, 10 mM EGTA, 10 mM HEPES, 4 mM MgCl₂,
558 0.3 mM GTP and 2 mM ATP-Na₂ (pH adjusted to 7.2 with KOH, 300 mOsm/l). All recordings

559 were performed at room temperature. Data were acquired using an Axopatch 200B (Axon
560 Instruments), low-pass filtered at 5 kHz and collected at 10 kHz using a Digidata 1322 A
561 digitizer (Axon Instruments). Once whole cell configuration was established, liquid junction
562 potential and capacitance transients were compensated. Resting membrane potential measured
563 in current clamp mode ($I = 0$) was stable and registered using the built-in voltmeter in the
564 Axopatch 200B. Input and series resistance were monitored during the experiment, and
565 recordings were excluded when any of these parameters changed by $>10\%$. Values obtained
566 were annotated in the laboratory protocol notebook. Recordings of total synaptic activity were
567 done for 2 min in a gap-free mode using Clampex 10.1 and analysis was performed offline
568 using Clampfit 10.1 (Axon Instruments) and Excel (Microsoft Corporation).

569

570 **Statistics.** GraphPad Prism (Version 9.0.0 (121) Graph-Pad Software Inc) was used for data
571 display and statistical analysis. We did not predetermine sample sizes. The Shapiro-Wilk test
572 was used to test for the normality of data. Parametric testing procedures (Student's *t*-test or one-
573 way analysis of variance (ANOVA) followed by Tukey's multiple comparison post-test when
574 many subgroups were compared) were applied for normally distributed data, otherwise
575 nonparametric tests were used (Mann-Whitney or Kruskal-Wallis tests followed by Dunn's
576 multiple-comparison post-test when many subgroups were compared). Total number of samples
577 (*n*) analysed in all experimental conditions (number of repeated measurements) is indicated in
578 figures legends. Results were presented as mean \pm SEM and statistical significance was set at
579 *P* values < 0.05 (two-tailed tests) (**P* <0.05 , ***P* <0.01 ; ****P* <0.001). In electrophysiology, for
580 non-normally distributed data Kolmogorov-Smirnov test was selected. Values of *P* < 0.05 were
581 considered statistically significant.

582

583 **Study approval.**

584 **Human brain autopsy.** Human brain tissues were obtained from the GIE NeuroCEB (Paris)
585 (<https://www.neuroceb.org/en/>), the Netherlands (Amsterdam) (www.brainbank.nl) and the
586 ULB LHNN (Brussels) Brain Banks. GIE NeuroCEB's Brain Bank procedures have been
587 reviewed and accepted by the Ethical Committee "Comité de Protection des Personnes Paris Ile
588 de France VI" and has been declared to the Ministry of Research and Higher Education as
589 requested by the French law. The Netherlands Brain Bank received permission to perform
590 autopsies and to use tissue and medical records from the Ethical Committee of the VU
591 University Medical Center. Tissues from the ULB LHNN Brain Bank were obtained in
592 compliance and following approval of the Ethical Committee of the Medical School of the Free
593 University of Brussels. An explicit informed consent had been signed by the patient or by the
594 next of kin, in the name of the patient for autopsy and use of their brain tissue for research
595 purposes. **Animals.** All animal procedures used in the study were carried out in accordance
596 with institutional and European guidelines as certified by the local Animal Ethics Committee.
597 Housing conditions were specified by the Belgian Law of 29 May 2013, regarding the
598 protection of laboratory animals (agreement and project numbers: LA2230419 / LA2230652
599 and 2018/UCL/MD/035).

600

601 **Author contributions**

602 N.P. supervised the project and edited the final version of the manuscript. N.P. and J-N.O.
603 designed the study. N.P., F.S-O., T.L., F.R. performed the research. A.K., K.L., F.L., E.B, B.S.,
604 C.D., P.B; and P.G. contributed the new reagents/analytic tools. N.P., F.S-O. and T.L., analysed
605 the data. N.P. and F.S-O. wrote the manuscript in consultation with J-N.O.

606

607 **Acknowledgments**

608 We thank the Fondation Louvain for a support to N.P. and the Chilean ANID “Becas Chile” for
609 a support to F.S-O, the Netherlands Brain Bank for providing us with human brain samples.
610 This work was supported by the Belgian Fonds pour la Recherche Scientifique, The Concerted
611 Research Actions, The Belgian Fonds de la Recherche Scientifique Médicale, the Queen
612 Elisabeth Medical Foundation and the Fondation pour la Recherche sur la Maladie
613 d’Alzheimer.

614

615 **References**

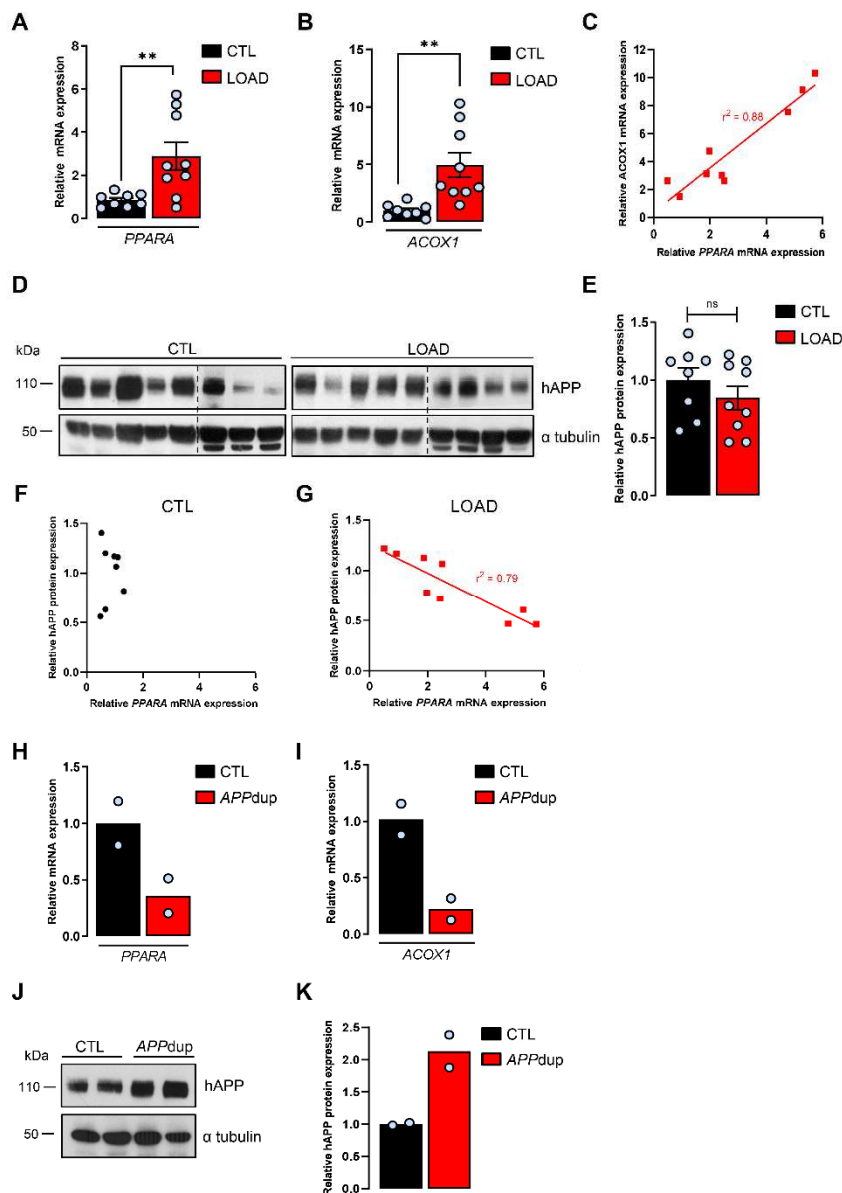
- 616 1. Lane CA, Hardy J, and Schott JM. Alzheimer's disease. *Eur J Neurol*. 2018;25(1):59-70.
617 2. DeTure MA, and Dickson DW. The neuropathological diagnosis of Alzheimer's disease.
618 *Molecular Neurodegeneration*. 2019;14(1):32.
619 3. Selkoe DJ. Alzheimer's disease is a synaptic failure. *Science*. 2002;298(5594):789-91.
620 4. Bellenguez C, Grenier-Boley B, and Lambert JC. Genetics of Alzheimer's disease: where we are,
621 and where we are going. *Curr Opin Neurobiol*. 2020;61:40-8.
622 5. Di Paolo G, and Kim TW. Linking lipids to Alzheimer's disease: cholesterol and beyond. *Nat Rev*
623 *Neurosci*. 2011;12(5):284-96.
624 6. Picard C, Julien C, Frappier J, Miron J, Theroux L, Dea D, et al. Alterations in cholesterol
625 metabolism-related genes in sporadic Alzheimer's disease. *Neurobiol Aging*. 2018;66:180 e1-
626 e9.
627 7. Spell C, Kölsch H, Lütjohann D, Kerksiek A, Hentschel F, Damian M, et al. SREBP-1a
628 Polymorphism Influences the Risk of Alzheimer's Disease in Carriers of the ApoE4 Allele.
629 *Dementia and Geriatric Cognitive Disorders*. 2004;18(3-4):245-9.
630 8. Brune S, Kolsch H, Ptok U, Majores M, Schulz A, Schlosser R, et al. Polymorphism in the
631 peroxisome proliferator-activated receptor alpha gene influences the risk for Alzheimer's
632 disease. *J Neural Transm (Vienna)*. 2003;110(9):1041-50.
633 9. Sjolander A, Minthon L, Bogdanovic N, Wallin A, Zetterberg H, and Blennow K. The PPAR-alpha
634 gene in Alzheimer's disease: lack of replication of earlier association. *Neurobiol Aging*.
635 2009;30(4):666-8.
636 10. Saez-Orellana F, Octave JN, and Pierrot N. Alzheimer's Disease, a Lipid Story: Involvement of
637 Peroxisome Proliferator-Activated Receptor alpha. *Cells*. 2020;9(5).
638 11. Bougarne N, Weyers B, Desmet SJ, Deckers J, Ray DW, Staels B, et al. Molecular Actions of
639 PPAR α in Lipid Metabolism and Inflammation. *Endocrine Reviews*. 2018;39(5):760-802.
640 12. Camandola S, and Mattson MP. Brain metabolism in health, aging, and neurodegeneration.
641 *EMBO J*. 2017;36(11):1474-92.
642 13. Snowden SG, Ebshiana AA, Hye A, An Y, Pletnikova O, O'Brien R, et al. Association between
643 fatty acid metabolism in the brain and Alzheimer disease neuropathology and cognitive
644 performance: A nontargeted metabolomic study. *PLOS Medicine*. 2017;14(3):e1002266.
645 14. Hardy J, and Escott-Price V. Genes, pathways and risk prediction in Alzheimer's disease. *Hum*
646 *Mol Genet*. 2019;28(R2):R235-R40.
647 15. D'Agostino G, Cristiano C, Lyons DJ, Citraro R, Russo E, Avagliano C, et al. Peroxisome
648 proliferator-activated receptor alpha plays a crucial role in behavioral repetition and cognitive
649 flexibility in mice. *Mol Metab*. 2015;4(7):528-36.
650 16. Roy A, Jana M, Corbett GT, Ramaswamy S, Kordower JH, Gonzalez FJ, et al. Regulation of cyclic
651 AMP response element binding and hippocampal plasticity-related genes by peroxisome
652 proliferator-activated receptor alpha. *Cell Rep*. 2013;4(4):724-37.
653 17. Pierrot N, Ris L, Stancu IC, Doshina A, Ribeiro F, Tyteca D, et al. Sex-regulated gene dosage
654 effect of PPARalpha on synaptic plasticity. *Life Sci Alliance*. 2019;2(2).
655 18. Bliss TV, and Collingridge GL. A synaptic model of memory: long-term potentiation in the
656 hippocampus. *Nature*. 1993;361(6407):31-9.
657 19. Heneka MT, and Landreth GE. PPARs in the brain. *Biochim Biophys Acta*. 2007;1771(8):1031-
658 45.
659 20. Chandra S, Roy A, Jana M, and Pahan K. Cinnamic acid activates PPARalpha to stimulate
660 lysosomal biogenesis and lower amyloid plaque pathology in an Alzheimer's disease mouse
661 model. *Neurobiol Dis*. 2019;124:379-95.
662 21. Luo R, Su LY, Li G, Yang J, Liu Q, Yang LX, et al. Activation of PPARA-mediated autophagy
663 reduces Alzheimer disease-like pathology and cognitive decline in a murine model. *Autophagy*.
664 2020;16(1):52-69.

- 665 22. de la Monte SM, and Wands JR. Molecular indices of oxidative stress and mitochondrial
666 dysfunction occur early and often progress with severity of Alzheimer's disease. *J Alzheimers*
667 *Dis.* 2006;9(2):167-81.
- 668 23. Pierrot N, Tyteca D, D'auria L, Dewachter I, Gailly P, Hendrickx A, et al. Amyloid precursor
669 protein controls cholesterol turnover needed for neuronal activity. *EMBO Mol Med.*
670 2013;5(4):608-25.
- 671 24. Zhang S, Hulver MW, McMillan RP, Cline MA, and Gilbert ER. The pivotal role of pyruvate
672 dehydrogenase kinases in metabolic flexibility. *Nutr Metab (Lond).* 2014;11(1):10.
- 673 25. Wang W, Zhao F, Ma X, Perry G, and Zhu X. Mitochondria dysfunction in the pathogenesis of
674 Alzheimer's disease: recent advances. *Mol Neurodegener.* 2020;15(1):30.
- 675 26. Kao YC, Ho PC, Tu YK, Jou IM, and Tsai KJ. Lipids and Alzheimer's Disease. *Int J Mol Sci.*
676 2020;21(4).
- 677 27. Rovelet-Lecrux A, Hannequin D, Raux G, Le Meur N, Laquerriere A, Vital A, et al. APP locus
678 duplication causes autosomal dominant early-onset Alzheimer disease with cerebral amyloid
679 angiopathy. *Nat Genet.* 2006;38(1):24-6.
- 680 28. Selkoe DJ, and Hardy J. The amyloid hypothesis of Alzheimer's disease at 25 years. *EMBO Mol*
681 *Med.* 2016.
- 682 29. Sleegers K, Brouwers N, Gijssels I, Theuns J, Goossens D, Wauters J, et al. APP duplication is
683 sufficient to cause early onset Alzheimer's dementia with cerebral amyloid angiopathy. *Brain.*
684 2006;129(Pt 11):2977-83.
- 685 30. Esquerda-Canals G, Montoliu-Gaya L, Güell-Bosch J, and Villegas S. Mouse Models of
686 Alzheimer's Disease. *Journal of Alzheimer's Disease.* 2017;57:1171-83.
- 687 31. Mucke L, Masliah E, Yu GQ, Mallory M, Rockenstein EM, Tatsuno G, et al. High-level neuronal
688 expression of abeta 1-42 in wild-type human amyloid protein precursor transgenic mice:
689 synaptotoxicity without plaque formation. *J Neurosci.* 2000;20(11):4050-8.
- 690 32. Johnson ECB, Ho K, Yu GQ, Das M, Sanchez PE, Djukic B, et al. Behavioral and neural network
691 abnormalities in human APP transgenic mice resemble those of App knock-in mice and are
692 modulated by familial Alzheimer's disease mutations but not by inhibition of BACE1. *Mol*
693 *Neurodegener.* 2020;15(1):53.
- 694 33. Jernberg JN, Bowman CE, Wolfgang MJ, and Scafidi S. Developmental regulation and
695 localization of carnitine palmitoyltransferases (CPTs) in rat brain. *J Neurochem.*
696 2017;142(3):407-19.
- 697 34. Kim YJ, Tu TH, Yang S, Kim JK, and Kim JG. Characterization of Fatty Acid Composition
698 Underlying Hypothalamic Inflammation in Aged Mice. *Molecules.* 2020;25(14).
- 699 35. Simon AM, Schiapparelli L, Salazar-Colocho P, Cuadrado-Tejedor M, Escribano L, Lopez de
700 Maturana R, et al. Overexpression of wild-type human APP in mice causes cognitive deficits
701 and pathological features unrelated to Abeta levels. *Neurobiol Dis.* 2009;33(3):369-78.
- 702 36. Gonzalez-Dominguez R, Garcia-Barrera T, Vitorica J, and Gomez-Ariza JL. Metabolomic
703 screening of regional brain alterations in the APP/PS1 transgenic model of Alzheimer's disease
704 by direct infusion mass spectrometry. *J Pharm Biomed Anal.* 2015;102:425-35.
- 705 37. Wojtowicz S, Strosznajder AK, Jezyna M, and Strosznajder JB. The Novel Role of PPAR Alpha in
706 the Brain: Promising Target in Therapy of Alzheimer's Disease and Other Neurodegenerative
707 Disorders. *Neurochem Res.* 2020;45(5):972-88.
- 708 38. Doshina A, Gourgue F, Onizuka M, Opsomer R, Wang P, Ando K, et al. Cortical cells reveal APP
709 as a new player in the regulation of GABAergic neurotransmission. *Sci Rep.* 2017;7(1):370.
- 710 39. Schlaepfer IR, and Joshi M. CPT1A-mediated Fat Oxidation, Mechanisms, and Therapeutic
711 Potential. *Endocrinology.* 2020;161(2).
- 712 40. Joshi M, Kim J, D'Alessandro A, Monk E, Bruce K, Elajaili H, et al. CPT1A Over-Expression
713 Increases Reactive Oxygen Species in the Mitochondria and Promotes Antioxidant Defenses in
714 Prostate Cancer. *Cancers (Basel).* 2020;12(11).
- 715 41. Das SK, Eder S, Schauer S, Diwoky C, Temmel H, Guertl B, et al. Adipose triglyceride lipase
716 contributes to cancer-associated cachexia. *Science.* 2011;333(6039):233-8.

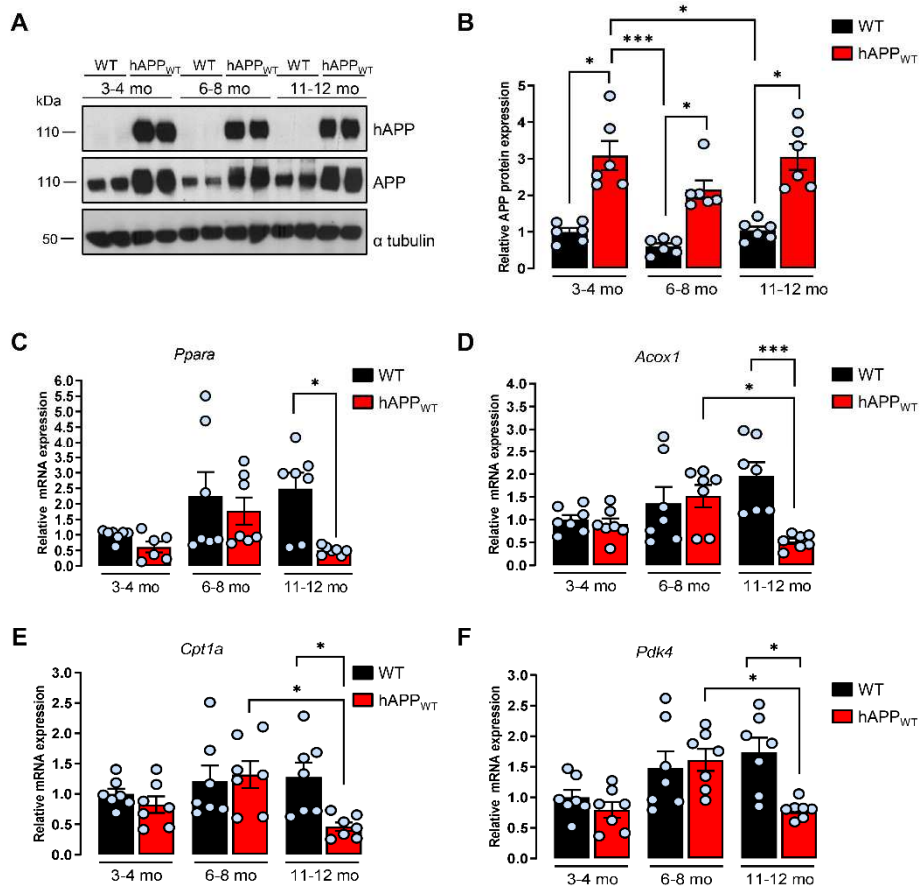
- 717 42. Lopez Sanchez MIG, Waugh HS, Tsatsanis A, Wong BX, Crowston JG, Duce JA, et al. Amyloid
718 precursor protein drives down-regulation of mitochondrial oxidative phosphorylation
719 independent of amyloid beta. *Sci Rep.* 2017;7(1):9835.
- 720 43. Rakhshandehroo M, Knoch B, Muller M, and Kersten S. Peroxisome proliferator-activated
721 receptor alpha target genes. *PPAR Res.* 2010;2010.
- 722 44. Kamenetz F, Tomita T, Hsieh H, Seabrook G, Borchelt D, Iwatsubo T, et al. APP processing and
723 synaptic function. *Neuron.* 2003;37(6):925-37.
- 724 45. Ting JT, Kelley BG, Lambert TJ, Cook DG, and Sullivan JM. Amyloid precursor protein
725 overexpression depresses excitatory transmission through both presynaptic and postsynaptic
726 mechanisms. *Proc Natl Acad Sci U S A.* 2007;104(1):353-8.
- 727 46. Manczak M, and Reddy PH. RNA silencing of genes involved in Alzheimer's disease enhances
728 mitochondrial function and synaptic activity. *Biochim Biophys Acta.* 2013;1832(12):2368-78.
- 729 47. Xu HE, Stanley TB, Montana VG, Lambert MH, Shearer BG, Cobb JE, et al. Structural basis for
730 antagonist-mediated recruitment of nuclear co-repressors by PPARalpha. *Nature.*
731 2002;415(6873):813-7.
- 732 48. Hoyer A, Bardenheuer HJ, Martin E, and Plaschke K. Amyloid precursor protein (APP) and its
733 derivatives change after cellular energy depletion. An in vitro-study. *J Neural Transm (Vienna).*
734 2005;112(2):239-53.
- 735 49. Pottier C, Wallon D, Lecrux AR, Maltete D, Bombois S, Jurici S, et al. Amyloid-beta protein
736 precursor gene expression in alzheimer's disease and other conditions. *J Alzheimers Dis.*
737 2012;28(3):561-6.
- 738 50. Van den Heuvel C, Blumbergs PC, Finnie JW, Manavis J, Jones NR, Reilly PL, et al. Upregulation
739 of amyloid precursor protein messenger RNA in response to traumatic brain injury: an ovine
740 head impact model. *Exp Neurol.* 1999;159(2):441-50.
- 741 51. Herbst-Robinson KJ, Liu L, James M, Yao Y, Xie SX, and Brunden KR. Inflammatory Eicosanoids
742 Increase Amyloid Precursor Protein Expression via Activation of Multiple Neuronal Receptors.
743 *Sci Rep.* 2015;5:18286.
- 744 52. Haga S, Akai K, and Ishii T. Demonstration of microglial cells in and around senile (neuritic)
745 plaques in the Alzheimer brain. An immunohistochemical study using a novel monoclonal
746 antibody. *Acta Neuropathol.* 1989;77(6):569-75.
- 747 53. Jonsson T, Stefansson H, Steinberg S, Jonsdottir I, Jonsson PV, Snaedal J, et al. Variant of TREM2
748 associated with the risk of Alzheimer's disease. *N Engl J Med.* 2013;368(2):107-16.
- 749 54. Sorbi S, Bird ED, and Blass JP. Decreased pyruvate dehydrogenase complex activity in
750 Huntington and Alzheimer brain. *Ann Neurol.* 1983;13(1):72-8.
- 751 55. Yellen G. Fueling thought: Management of glycolysis and oxidative phosphorylation in
752 neuronal metabolism. *J Cell Biol.* 2018;217(7):2235-46.
- 753 56. Sugden MC, Kraus A, Harris RA, and Holness MJ. Fibre-type specific modification of the activity
754 and regulation of skeletal muscle pyruvate dehydrogenase kinase (PDK) by prolonged
755 starvation and refeeding is associated with targeted regulation of PDK isoenzyme 4 expression.
756 *Biochem J.* 2000;346 Pt 3:651-7.
- 757 57. Berger J, Dorninger F, Forss-Petter S, and Kunze M. Peroxisomes in brain development and
758 function. *Biochim Biophys Acta.* 2016;1863(5):934-55.
- 759 58. Yao J, Rettberg JR, Klosinski LP, Cadenas E, and Brinton RD. Shift in brain metabolism in late
760 onset Alzheimer's disease: implications for biomarkers and therapeutic interventions. *Mol*
761 *Aspects Med.* 2011;32(4-6):247-57.
- 762 59. Lott IT, and Head E. Dementia in Down syndrome: unique insights for Alzheimer disease
763 research. *Nat Rev Neurol.* 2019;15(3):135-47.
- 764 60. Dierssen M, Fructuoso M, Martinez de Lagran M, Perluigi M, and Barone E. Down Syndrome Is
765 a Metabolic Disease: Altered Insulin Signaling Mediates Peripheral and Brain Dysfunctions.
766 *Front Neurosci.* 2020;14:670.
- 767 61. Chapel-Crespo CC, Lala S, and Prasun P. Severe Brain Malformations in an Infant With Pyruvate
768 Dehydrogenase Deficiency and Down Syndrome. *Pediatr Neurol.* 2017;75:101-2.

- 769 62. Song HJ, Park J, Seo SR, Kim J, Paik SR, and Chung KC. Down syndrome critical region 2 protein
770 inhibits the transcriptional activity of peroxisome proliferator-activated receptor beta in
771 HEK293 cells. *Biochem Biophys Res Commun.* 2008;376(3):478-82.
- 772 63. Cimini A, Moreno S, D'Amelio M, Cristiano L, D'Angelo B, Falone S, et al. Early biochemical and
773 morphological modifications in the brain of a transgenic mouse model of Alzheimer's disease:
774 a role for peroxisomes. *J Alzheimers Dis.* 2009;18(4):935-52.
- 775 64. Fanelli F, Sepe S, D'Amelio M, Bernardi C, Cristiano L, Cimini A, et al. Age-dependent roles of
776 peroxisomes in the hippocampus of a transgenic mouse model of Alzheimer's disease. *Mol*
777 *Neurodegener.* 2013;8:8.
- 778 65. Bielarczyk H, Jankowska-Kulawy A, Hofling C, Ronowska A, Gul-Hinc S, Rossner S, et al.
779 AbetaPP-Transgenic 2576 Mice Mimic Cell Type-Specific Aspects of Acetyl-CoA-Linked
780 Metabolic Deficits in Alzheimer's Disease. *J Alzheimers Dis.* 2015;48(4):1083-94.
- 781 66. Jha MK, Jeon S, and Suk K. Pyruvate Dehydrogenase Kinases in the Nervous System: Their
782 Principal Functions in Neuronal-glia Metabolic Interaction and Neuro-metabolic Disorders.
783 *Curr Neuropharmacol.* 2012;10(4):393-403.
- 784 67. Edmond J. Energy metabolism in developing brain cells. *Can J Physiol Pharmacol.* 1992;70
785 Suppl:S118-29.
- 786 68. Hall CN, Klein-Flugge MC, Howarth C, and Attwell D. Oxidative phosphorylation, not glycolysis,
787 powers presynaptic and postsynaptic mechanisms underlying brain information processing. *J*
788 *Neurosci.* 2012;32(26):8940-51.
- 789 69. Priller C, Bauer T, Mitteregger G, Krebs B, Kretzschmar HA, and Herms J. Synapse formation
790 and function is modulated by the amyloid precursor protein. *J Neurosci.* 2006;26(27):7212-21.
- 791 70. Czczor JK, Genders AJ, Aston-Mourney K, Connor T, Hall LG, Hasebe K, et al. APP deficiency
792 results in resistance to obesity but impairs glucose tolerance upon high fat feeding. *J*
793 *Endocrinol.* 2018;237(3):311-22.
- 794 71. Gratacos-Batlle E, Yefimenko N, Cascos-Garcia H, and Soto D. AMPAR interacting protein
795 CPT1C enhances surface expression of GluA1-containing receptors. *Front Cell Neurosci.*
796 2014;8:469.
- 797 72. Santos MJ, Quintanilla RA, Toro A, Grandy R, Dinamarca MC, Godoy JA, et al. Peroxisomal
798 proliferation protects from beta-amyloid neurodegeneration. *J Biol Chem.*
799 2005;280(49):41057-68.
- 800 73. Cimini A, Benedetti E, D'Angelo B, Cristiano L, Falone S, Di Loreto S, et al. Neuronal response
801 of peroxisomal and peroxisome-related proteins to chronic and acute Abeta injury. *Curr*
802 *Alzheimer Res.* 2009;6(3):238-51.
- 803 74. Corbett GT, Gonzalez FJ, and Pahan K. Activation of peroxisome proliferator-activated receptor
804 alpha stimulates ADAM10-mediated proteolysis of APP. *Proc Natl Acad Sci U S A.*
805 2015;112(27):8445-50.
- 806 75. Melis M, Scheggi S, Carta G, Madeddu C, Lecca S, Luchicchi A, et al. PPARalpha regulates
807 cholinergic-driven activity of midbrain dopamine neurons via a novel mechanism involving
808 alpha7 nicotinic acetylcholine receptors. *J Neurosci.* 2013;33(14):6203-11.
- 809 76. Pousinha PA, Mouska X, Raymond EF, Gwizdek C, Dhib G, Poupon G, et al. Physiological and
810 pathophysiological control of synaptic GluN2B-NMDA receptors by the C-terminal domain of
811 amyloid precursor protein. *Elife.* 2017;6.
- 812 77. Hefter D, Ludewig S, Draguhn A, and Korte M. Amyloid, APP, and Electrical Activity of the Brain.
813 *Neuroscientist.* 2020;26(3):231-51.
- 814 78. Cabrejo L, Guyant-Marechal L, Laquerriere A, Vercelletto M, De la Fourniere F, Thomas-
815 Anterion C, et al. Phenotype associated with APP duplication in five families. *Brain.*
816 2006;129(Pt 11):2966-76.
- 817 79. Menendez M. Down syndrome, Alzheimer's disease and seizures. *Brain Dev.* 2005;27(4):246-
818 52.

- 819 80. Born HA, Kim JY, Savjani RR, Das P, Dabaghian YA, Guo Q, et al. Genetic suppression of
820 transgenic APP rescues Hypersynchronous network activity in a mouse model of Alzheimer's
821 disease. *J Neurosci.* 2014;34(11):3826-40.
- 822 81. Lee SS, Pineau T, Drago J, Lee EJ, Owens JW, Kroetz DL, et al. Targeted disruption of the alpha
823 isoform of the peroxisome proliferator-activated receptor gene in mice results in abolishment
824 of the pleiotropic effects of peroxisome proliferators. *Mol Cell Biol.* 1995;15(6):3012-22.
- 825

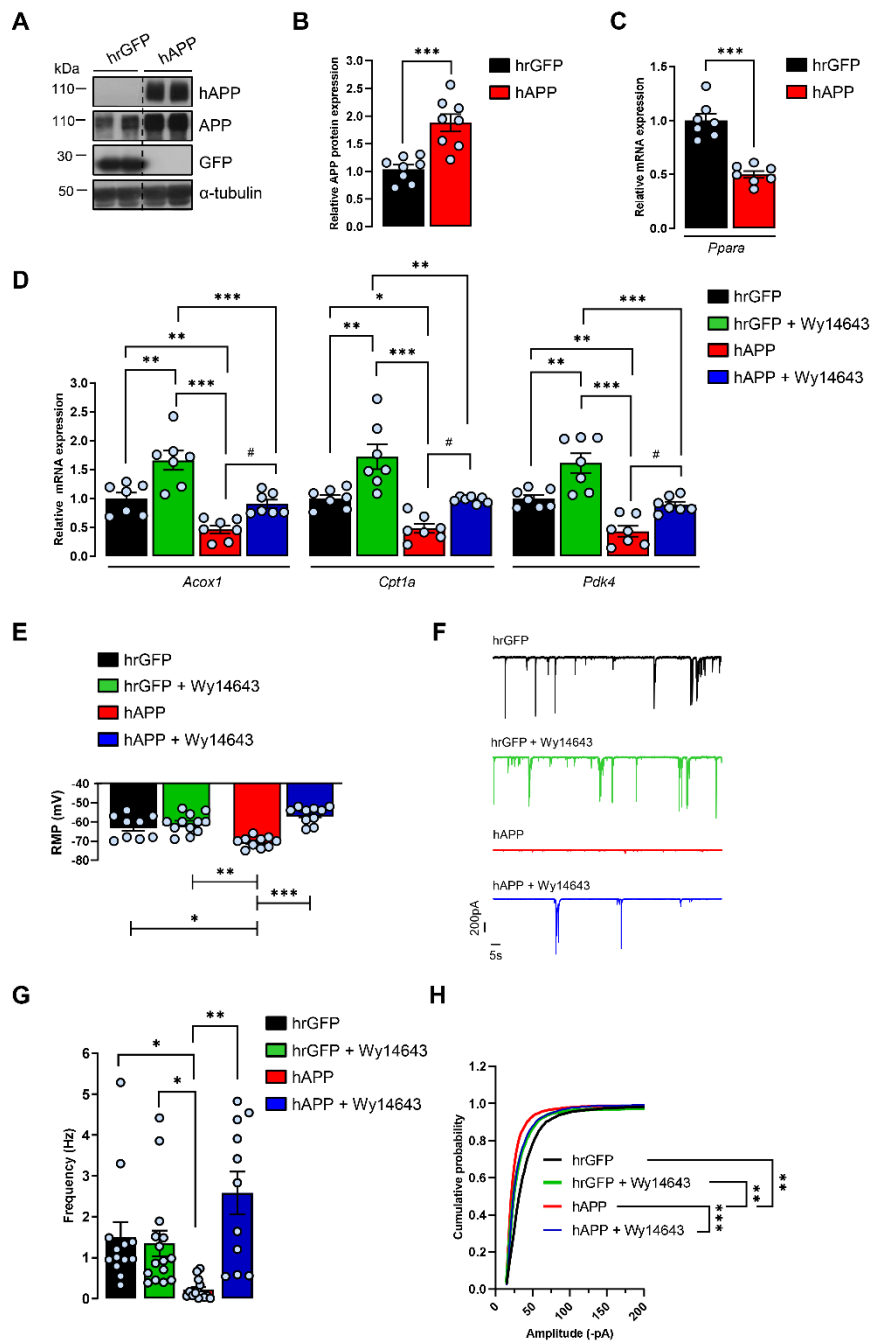


827
 828 **Figure 1. *PPARA* expression and *PPAR α downstream target genes in brains from patients***
 829 **with Alzheimer disease.** Frontal cortex of postmortem human brain tissues from late-onset
 830 (LOAD, $n = 9$) and early-onset Alzheimer disease cases with an *APP* duplication locus
 831 (*APPdup*, $n = 2$) and respective control subjects (CTL in LOAD and *APPdup* cases, $n = 8$ and
 832 2, respectively) were analysed. (**A**, **B**, **H** and **I**) Quantitative real time PCR analyses for *PPARA*
 833 and *ACOX1* mRNA levels. Results were normalized to *ACTB* mRNA and relative differences
 834 are expressed according to respective CTL as mean \pm SEM (LOAD: *PPARA* mRNA, $P = 0.009$,
 835 *ACOX1* mRNA, $P = 0.003$; Student's t-test). (**C**) mRNA correlation between *ACOX1* and
 836 *PPARA* in LOAD. (**D**, **J**) Human APP (hAPP) expression in human brain lysates by
 837 immunoblot analysis (see complete unedited blots in the supplemental material). (**E**, **K**)
 838 Relative density of hAPP expression compared with α -tubulin. Results were normalized
 839 compared to respective CTL and are shown as mean \pm SEM. A Student's t-test (LOAD: hAPP
 840 protein, $P = 0.0608$) was used to assess significance of the mean. (**F**, **G**) Quantification of hAPP
 841 densitometry arbitrary units indicating an inverse correlation between hAPP expression and
 842 *PPARA* levels in LOAD. ** $P < 0.01$ and non-significant (ns) $P > 0.05$.



843
 844 **Figure 2. Human APP expression decreases *Ppara* expression and PPAR α downstream**
 845 **target genes in old mice.** Brain frontal cortex tissues from transgenic mice overexpressing non-
 846 non-mutated human APP (hAPP_{WT}) and wild type (WT) littermates were analysed at 3-4, 6-8 and
 847 11-12 months old (mo). (A) The expression of hAPP was investigated in mice brain lysates (n
 848 = 6 of each) by immunoblot analysis (see complete unedited blots in the supplemental material)
 849 with the specific WO2 antibody recognizing hAPP and anti-APP C-terminal antibody
 850 recognizing both hAPP and endogenous APP (APP). Blots were further probed using anti- α -
 851 tubulin antibody. (B) Relative density of APP expression was compared with α -tubulin. Results
 852 were normalized compared to 3-4 mo WT and are shown as mean \pm SEM. A Kruskal-Wallis
 853 test followed by Dunn's multiple comparisons post-test was used to assess significance of the
 854 mean (APP protein expression at 3-4, 6-8 and 11-12 mo, $P < 0.05$). (C-F) Quantitative real time
 855 PCR analyses (n = 7 of each) for *Ppara*, *Acox1*, *Cpt1a* and *Pdk4* mRNA levels. Results were
 856 normalized to *Rpl32* mRNA, compared to 3-4 mo WT and shown as mean \pm SEM. A Kruskal-
 857 Wallis test followed by Dunn's multiple comparisons post-test was used to assess significance
 858 of the mean (11-12 mo hAPP_{WT} mice: *Ppara* mRNA, $P = 0.012$, *Acox1* mRNA, $P = 0.0008$,
 859 *Cpt1a* mRNA, $P = 0.031$; *Pdk4* mRNA, $P = 0.022$), * $P < 0.05$, *** $P < 0.001$.

860
 861



862
 863 **Figure 3. Pharmacological PPAR α activation with the Wy14643 prevents human APP-**
 864 **induced decreases in the expression of PPAR α target genes and synaptic activity in**
 865 **cortical cultures.** Primary cultures of rat cortical cells expressing human recombinant GFP
 866 (hrGFP) or APP (hAPP) treated (+) or not (-) with 10 μ M PPAR α agonist Wy14643 for 24h at
 867 13-14 DIV. **(A)** Representative immunoblot of cell lysates (4 independent experiments). The
 868 lanes were run on the same gel but were noncontiguous. **(B)** APP expression / α tubulin ratios
 869 (n = 8 of each analysed in 4 independent experiments) compared to hrGFP control cells (mean
 870 \pm SEM); Student's t-test (APP protein, $P = 0.0608$). **(C, D)** Real time PCR analyses for *Ppara*,
 871 *Acox1*, *Cpt1a* and *Pdk4* mRNA levels (n = 7 of each analysed in 4 independent experiments).
 872 Results were normalized to *Rpl32* mRNA and compared to respective untreated (-) hrGFP
 873 control cells. Results are shown as mean \pm SEM; one-way ANOVA followed by Tukey's
 874 multiple comparisons test ((-) hAPP vs (-) hrGFP: *Ppara* mRNA, $P < 0.0001$, *Acox1* mRNA,

875 $P = 0.009$, *Cpt1a* mRNA, $P = 0.026$; *Pdk4* mRNA, $P = 0.003$; (+) hAPP vs (-) hAPP: *Acox1*
876 mRNA, $P = 0.039$, *Cpt1a* mRNA, $P = 0.035$; *Pdk4* mRNA, $P = 0.022$). (E) Resting membrane
877 potential (RMP) (n = 13-15 cells per group analysed in 5 independent experiments). (F)
878 Representative traces of total synaptic activity and (G) mean values of synaptic events
879 frequency (n = 15-24 cells per group analysed in 6 independent experiments). (H) Cumulative
880 probability plot of the amplitude distribution (n = 15-25 cells per group in 6 independent
881 experiments). (E - H) Brown-Forsythe and Welch ANOVA tests followed by Dunnett's T3
882 multiple comparisons test. * $P < 0.05$, ** $P < 0.01$, *** $P < 0.001$, # $P < 0.05$.

883

884

885

886

887

888

889

890

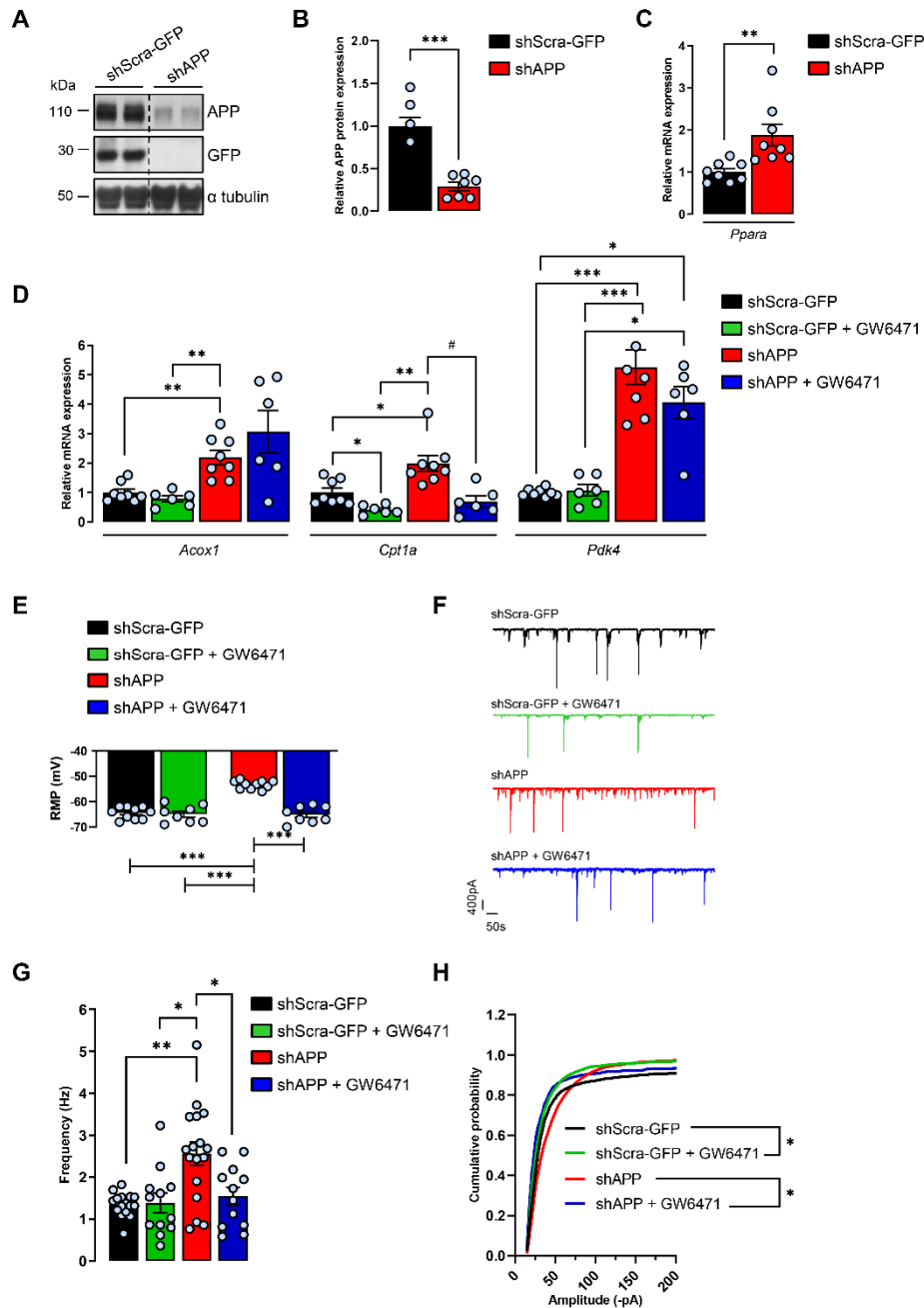
891

892

893

894

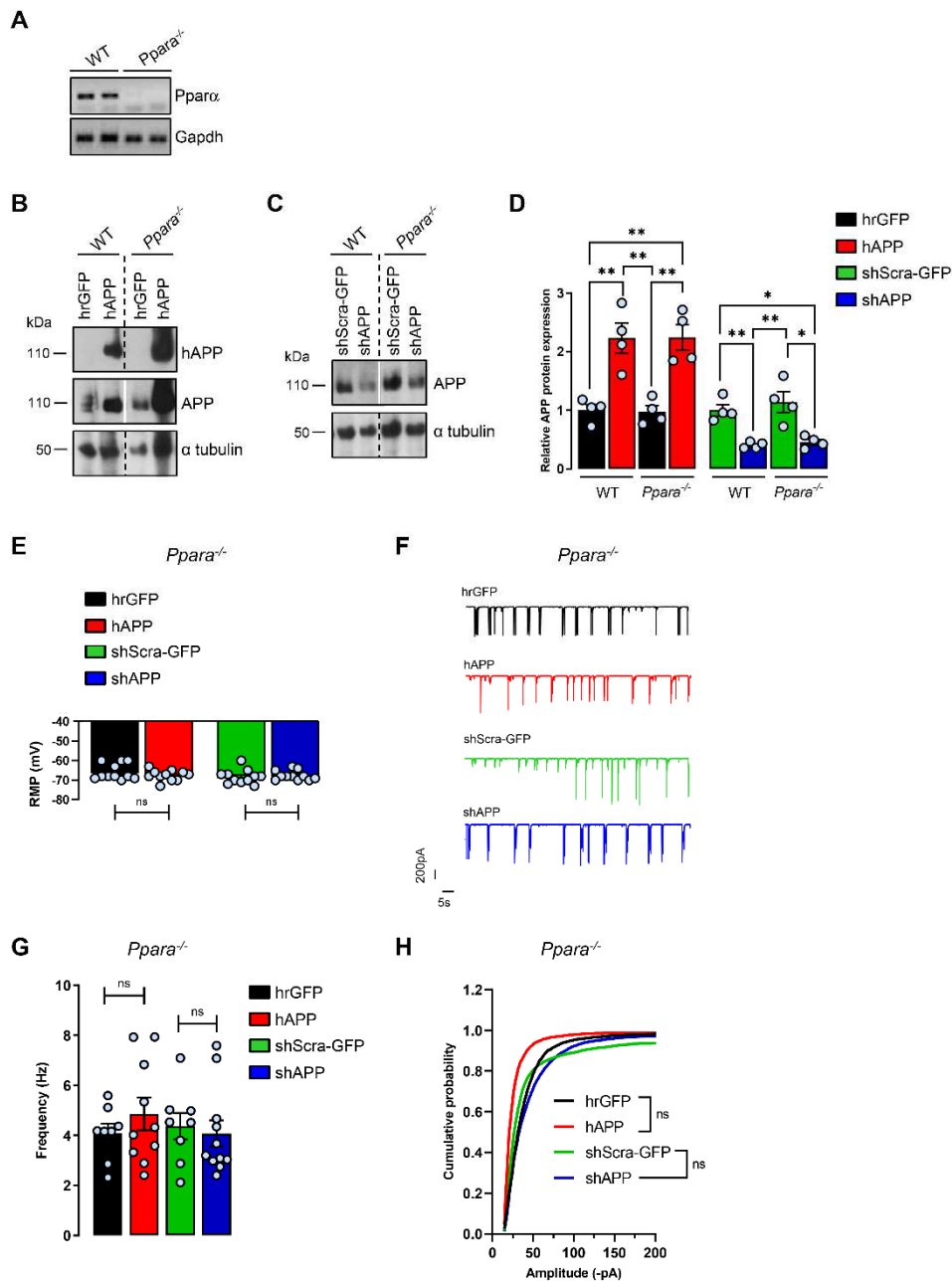
895



896
 897 **Figure 4. Pharmacological PPAR α inhibition with the GW6471 prevents APP**
 898 **knockdown-induced increases in the expression of PPAR α target genes and synaptic**
 899 **activity in cortical cultures.** Primary cultures of rat cortical cells expressing a shRNA targeting
 900 endogenous APP (shAPP) or a scrambled shRNA encoding GFP (shScra-GFP). At 13-14 DIV,
 901 cells were treated (+) or not (-) with PPAR α antagonist GW6471 for 24h. (A) Representative
 902 immunoblot of cell lysates, 4 independent experiments (the lanes were run on the same gel but
 903 were noncontiguous). (B) APP expression / α tubulin ratios (n = 7 of each analysed in 4
 904 independent experiments), mean \pm SEM; Student's t-test (APP protein, $P < 0.001$). (C and D)
 905 Real time PCR analyses for *Ppara*, *Acox1*, *Cpt1a* and *Pdk4* mRNA levels (n = 6-8 for each
 906 condition analysed in 6 independent experiments). Results were normalized to *Rpl32* mRNA
 907 and compared to respective untreated (-) shScra-GFP control cells. Results are shown as mean
 908 \pm SEM; Brown-Forsythe and Welch ANOVA tests followed by Dunnett's T3 multiple
 909 comparisons test ((-) shAPP vs (-) shScra-GFP: *Ppara* mRNA, $P = 0.006$, *Acox1* mRNA, $P =$

910 0.008, *Cpt1a* mRNA, $P = 0.043$; *Pdk4* mRNA, $P = 0.0009$; (+) shScra-GFP vs (-) shScra-GFP:
911 *Cpt1a* mRNA, $P = 0.026$; (+) shAPP vs (-) shAPP: *Cpt1a* mRNA, $P = 0.010$). **(E)** Resting
912 membrane potential (RMP) (n = 8-10 cells per group analysed in 3 independent experiments).
913 **(F)** Representative traces of total synaptic activity and **(G)** mean values of synaptic events
914 frequency (n = 12-17 cells per group analysed in 6 independent experiments). **(H)** Cumulative
915 probability plot of the amplitude distribution (n = 15-27 cells per group in 7 independent
916 experiments). **(E - H)** Brown-Forsythe and Welch ANOVA tests followed by Dunnett's T3
917 multiple comparisons test. * $P < 0.05$, ** $P < 0.01$, *** $P < 0.001$, # $P < 0.05$.

918
919
920
921
922
923
924
925
926
927
928
929
930



931
 932 **Figure 5. Control of synaptic activity by APP in cortical cultures disappears in absence of**
 933 **PPAR α .** Primary cultures of mouse cortical cells prepared from wild type (WT) and *Ppara*
 934 deficient (*Ppara*^{-/-}) mice and infected with recombinant adenoviruses encoding human
 935 recombinant GFP (hrGFP) or APP (hAPP) proteins or with lentiviruses encoding a shRNA
 936 construct designed to target endogenous APP (shAPP) or a scrambled shRNA encoding GFP
 937 (shScra-GFP). (A) At 13-14 DIV, absence of PPAR α expression in cultured cells was assessed
 938 by measuring *Ppara* mRNA levels by semi-quantitative RT-PCR. (B, C) Representative
 939 immunoblots of cell lysates, 3 independent experiments (the lanes were run on the same gel but
 940 were noncontiguous). The expression of hAPP was monitored with the specific WO2 antibody
 941 recognizing hAPP and anti-APP C-terminal antibody recognizing both hAPP and endogenous
 942 APP (APP). Immunoblots were further probed using anti-GFP and - α tubulin antibodies. (D)
 943 APP expression / α tubulin ratios (n = 4 of each) compared to hrGFP or shScra-GFP WT cells
 944 (mean \pm SEM); One-way ANOVA followed by Tukey's multiple comparisons test (APP

945 protein: WT and *Ppara*^{-/-} hAPP $P = 0.002$; WT and *Ppara*^{-/-} shAPP, $P = 0.008$ and $P = 0.015$,
946 respectively). **(E)** Resting membrane potential (RMP) measured in WT and *Ppara*^{-/-} transduced
947 neurons (n = 11 cells per group analysed in 3 independent experiments). **(F)** Representative
948 traces of total synaptic activity and **(G)** mean values of synaptic events frequency (n = 8-11
949 cells per group analysed in 3 independent experiments). **(H)** Cumulative probability plot of the
950 amplitude distribution (n = 10-20 cells per group in 3 independent experiments) measured in
951 WT and *Ppara*^{-/-} transduced neurons. **(E - H)** Brown-Forsythe and Welch ANOVA tests
952 followed by Dunnett's T3 multiple comparisons test. * $P < 0.05$, ** $P < 0.01$, *** $P < 0.001$ and
953 non-significant (ns) $P > 0.05$.

954